Tracking Control of a Quadrotor UAV by Using Inertial Vector Measurements

Eduardo Espíndola and Yu Tang

***Abstract*—In this paper the tracking controller for a quadrotor unmanned aerial vehicle (UAV) is designed. The controller consists of an outer saturated position control loop and an inner attitude control loop. The outer position control defines a singularity-free thrust direction that ensures global exponential tracking. The inner attitude control, which requires only inertial vector measurements of at least two known noncolinear inertial reference vectors and gyro-rate measurements, is designed to track the desired attitude required for the position tracking. Semiglobal exponential stability of the overall system is ensured using Lyapunov analysis. Numerical simulations are provided to illustrate the main results and verify the robustness of the proposed controller under noisy measurements and parametric uncertainty.**

***Index Terms*—Exponential tracking, inertial measurements, gyro bias, nonlinear control, quadrotor UAV.**

I. Introduction

In the last two decades, control of unmanned aerial vehicles (UAVs) has been a rapidly growing research area. In particular, the full autonomy of these vehicles is pursued intensively due to potential applications in diverse area [1]–[3]. Within a variety of UAVs, vertical take-off and landing (VTOL) vehicles, e.g. quadrotors, have drawn particular attention for their versatility in applications and challenges posed in theory due to the subactuation nature [4]–[9]. To address this challenge, *vectored thrust* approach has been proposed in which the propulsive thrust vector in the body-fixed frame is first determined by an outer translational control loop through a desired attitude, then the desired attitude is tracked in the rotational subsystem by an inner torque control loop [10]–[12]. To avoid the singularity issue in the position controller, saturation control technique is commonly employed [13]. The stability of the overall system is then established by the Lyapunov analysis of cascade systems [14]–[16].

Notwithstanding the important advances, most of existing work assumes attitude measurements available in terms of rotation matrix [12], [16], unit quaternion [11], [17], or Euler angles [18], [19] in the control design. However, attitude is not measured directly but commonly reconstructed by an observer from inertial measurements provided by inertial measurement units (IMU) or CCD cameras [20], [21]. A few work has been reported for UAV position regulation [22] using directly the vector measurements.

This work presents the design of a tracking controller for a quadrotor UAV. The outer translational control loop employs the vectored thrust approach, while the inner rotational control loop is devised using alignment errors between vector measurements of at least two known noncolinear inertial reference vectors and the desired directional vectors determined by the desired attitude and the inertial reference vectors. Therefore, no attitude description nor its measurements are needed, but only vector and gyro-rate measurements are used to implement the attitude control. In addition, a saturated control is proposed for the translational controller, designed to avoid singularities in the thrust vector. The overall system is analyzed utilizing Lyapunov stability theory, and semiglobal exponential stability is achieved. The main contribution of this work is a modular design of a trajectory tracking controller for UAVs using only vector and biased gyro-rate measurements for the inner attitude control loop and the establishment of the semiglobal exponential stability of the overall system. To the best of our knowledge, this is the first result reported in the literature for UAV tracking using vector and biased gyro measurements with semiglobal exponential stability. In addition, for typical applications of a quadrotor such as position regulation, no linear velocity is need for controller implementation. A previous result was presented in [23] to address the attitude control of a rigid body using quaternion representation without position tracking.

The rest of the paper is organized as follows. Section II gives preliminaries, including the notation, rotational and translational motion equations of a UAV and the onboard measurement description. In Section III the tracking problem is formulated, and the desired attitude is defined in terms of the thrust vector and the desired yaw angle to track a desired trajectory. In Section IV the position control is first designed ignoring the coupling with the rotational dynamics, then the attitude control using inertial vector measurements and a gyro-bias observer are devised. The attitude tracking objective is stated as an alignment problem between vector measurements of at least two known noncolinear inertial reference vectors and the desired directional vectors determined by the desired attitude and the inertial reference vectors. Alignment errors are defined and their properties, including a novel relationship between the attitude error and alignment error (item (4) of Lemma 4.4), instrument for achieving semiglobal exponential stability of the overall system are summarized. At last, the overall system, consisting of the position controller, the attitude controller, and the gyro-bias observer, is analyzed to ensure the almost semiglobal exponential stability. Section V presents numerical simulations to illustrate the theoretical results and verify robustness of the tracking controller under noisy measurements and parametric uncertainty. Section VI

E. Espíndola (e-mail: eespindola@comunidad.unam.mx) and Y. Tang (corresponding author, e-mail: tang@unam.mx) are with the Faculty of Engineering, National Autonomous University of Mexico, Juriquilla, QRO, 76230, Mexico.

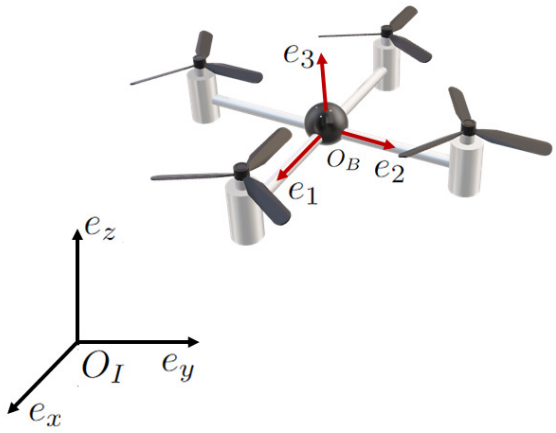

Fig. 1. Reference frames of the quadrotor UAV.

provides conclusion remarks. Appendix A gives the proof of Lemma 4.4.

II. Preliminaries

A. Notation

Vector norm $\|u\| = (u^T u)^{1/2}, \forall u \in \mathbb{R}^3$ and matrix norm $\|A\| = \lambda_{\max}^{1/2}(A^T A), \forall A \in \mathbb{R}^{n\times m}$ are used. The Frobenius norm is $\|A\|_F = \mathrm{tr}^{1/2}(A^T A), \forall A \in \mathbb{R}^{n\times n}$, with $\mathrm{tr}(\cdot)$ denoting the matrix trace. If matrix A is symmetric, $A = A^T > 0$ indicates a positive definite matrix, $\lambda_{\max}(A)$ and $\lambda_{\min}(A)$ are its maximum and minimum eigenvalues, respectively. I_n denotes the identity matrix of $n \times n$, $0_{n\times m}$ a zero matrix of $n \times m$. The map *wedge* $(\cdot)^\wedge : \mathbb{R}^3 \to \mathfrak{so}(3)$ is an isomorphism between $\mathbb{R}^3$ and the space of the skew-symmetric matrices $\mathfrak{so}(3) := \{A \in \mathbb{R}^{3\times 3} \mid A^T = -A\}$. The inverse map *vee* is given by $(\cdot)^\vee : \mathfrak{so}(3) \to \mathbb{R}^3$. The cross-product is $u^\wedge v = u \times v$, $\forall u, v \in \mathbb{R}^3$. A unit sphere of dimension $n-1$ embedded in space $\mathbb{R}^n$ is denoted by $\mathcal{S}^{n-1} := \{u \in \mathbb{R}^n | u^T u = 1\}$, while a $\mathbb{R}^n$-embedded ball of radius r is expressed as $B_r := \{u \in \mathbb{R}^n \mid \|u\| \le r\}$.

B. Quadrotor Model

Consider the body frame $\mathbf{B} = \{O_B, \{e_1, e_2, e_3\}\}$ with the origin O_B attached to the center of mass of the rigid body and an inertial frame $\mathbf{I} = \{O_I, \{e_x, e_y, e_z\}\}$ as shown in Fig. 1. The attitude of the body frame relative to the inertial frame is then fully defined by the rotation matrix $R \in SO(3) := \{R \in \mathbb{R}^{3\times 3} \mid R^T R = RR^T = I_3, \det(R) = 1\}$.

The motion equations of a quadrotor UAV are as follows

$$\dot{x} = v, \tag{1}$$
$$m\dot{v} = -mge_z + fRe_z + f_d, \tag{2}$$
$$\dot{R} = R(\omega)^\wedge, \tag{3}$$
$$M\dot{\omega} = (M\omega)^\wedge \omega + \tau + \tau_d, \tag{4}$$

where $(x, v) \in \mathbb{R}^3 \times \mathbb{R}^3$ are respectively the position and linear velocity of origin O_B, expressed in the inertial frame, $(R, \omega) \in SO(3) \times \mathbb{R}^3$ are the attitude and body-fixed angular velocity of the quadrotor, $(f, \tau) \in \mathbb{R} \times \mathbb{R}^3$ are the thrust force and the control torque expressed in the body-fixed frame $\mathbf{B}$, and $(f_d, \tau_d) \in \mathbb{R}^3 \times \mathbb{R}^3$ are the external disturbances, such as aerodynamic effects, unmodeled dynamics, and torque disturbances. Scalar $m > 0$ denotes the mass of the UAV, $M = M^T \in \mathbb{R}^{3\times 3}$ denotes the positive definite inertia matrix and $e_z = [0, 0, 1]^T$ represents the direction of the z -axis of the inertial frame, expressed in the body-fixed frame $\mathbf{B}$.

C. Measurements

The vehicle is assumed to be equipped with sensors that measure the state (x, v) expressed in $\mathbf{I}$, such as the GPS sensor in outdoor applications or digital cameras for indoor applications. In addition, the vehicle has access to the vector measurements $v_i \in \mathcal{S}^2$ in the body frame of $n \ge 2$ known constant reference vectors in the inertial frame $r_i \in \mathcal{S}^2$ as

$$v_i = R^T r_i, \quad i = 1, 2, \cdots, n. \tag{5}$$

Inertial Measurements Units (IMU) and CCD cameras are typical low-cost sensors used in UAVs that provide vector measurements.

The angular velocity is provided by a gyroscope. MEMS-technology based gyroscopes have a relatively large bias compared to high-precision gyroscopes, which must be corrected for control purpose. Therefore angular-velocity measurement ω_g is as follows

$$\omega_g = \omega + b, \tag{6}$$

where $b \in \mathbb{R}^3$ denotes gyro bias.

The following assumptions are made for the control design.

- Assumption A1: Among the n known constant inertial reference vectors, there are at least two noncollinear vectors.
- Assumption A2: Gyro bias b is a constant unknown vector that satisfies $\|b\| \le \mu_b$, for some $\mu_b > 0$ known.

III. Control Problem Statement

Given a desired position trajectory $x(t) \in \mathbb{R}^3$ and a desired yaw angle $\psi_d(t) \in \mathbb{R}$, which are assumed to be sufficiently smooth, define the position-tracking errors

$$\tilde{x} = x - x_d, \tag{7}$$
$$\tilde{v} = v - \dot{x}_d. \tag{8}$$

Their dynamics, by the translational motion equations (1)-(2) and ignoring the external disturbances, is

$$\dot{\tilde{x}} = \tilde{v}, \tag{9}$$
$$\begin{aligned} m\dot{\tilde{v}} &= -mge_z + fRe_z - m\ddot{x}_d \\ &= -mge_z - m\ddot{x}_d + fR_d e_z + f\left(R - R_d\right)e_z, \end{aligned} \tag{10}$$

where $R_d \in SO(3)$ is the desired attitude to be determined.

Note that the actuation mechanism is based on the thrust vector $fRe_z \in \mathbb{R}^3$, where the unit vector $Re_z \in \mathcal{S}^3$ gives the thrust direction to guide the UAV to track the desired position trajectory, while the thrust force f provides the thrust magnitude. Note that the thrust direction constraints the desired configurations for the rotational dynamics leaving the yaw

angle $\psi \in \mathbb{R}$ the only degree of freedom that can be controlled regardless of the position. Note also when $R = R_d$ the equilibrium $(\tilde{x}, \tilde{v}) = 0_{6\times 1}$ of the translational error dynamics (9)-(10) can be globally stabilized using thrust vector fR_de_z, giving rise to the two-stage control design strategy [10], [12], [18], [24], where an outer translational control loop is designed to follow the desired trajectory and determines the thrust direction and magnitude in the first stage, and an inner attitude control is designed to track the desired thrust direction in the second stage. The desired attitude trajectory can be computed as [13]

$$R_d := [c_1\ c_2\ c_3], \quad \omega_d = \left(R_d^T \dot{R}_d\right)^\vee, \tag{11}$$

where $c_1,\ c_2,\ c_3 \in \mathcal{S}^2$ are the column vectors of R_d given by

$$c_3 = \frac{T}{\|T\|},\ c_2 = \frac{c_3^\wedge c_d}{\|c_3^\wedge c_d\|},\ c_1 = c_2^\wedge c_3,$$

being $c_d = [\cos(\psi_d(t)), \sin(\psi_d(t)), 0]^T$ the desired yaw direction, and $T \in \mathbb{R}^3$, the thrust vector. The thrust force is obtained by $f = \|T\|$

Thus the control objective is to design a control law for the thrust vector T and hence the thrust force f and torque τ such that $(\tilde{x},\ \tilde{v}) \to 0_{6\times 1}$ and $(\psi - \psi_d, \dot{\psi} - \dot{\psi}_d) \to 0_{2\times 1}$ with all signals bounded.

It is clear that (11) is valid only when $\|T\| \neq 0$ and c_3, c_d are noncollinear. Both conditions can be ensured by designing a saturated control thrust vector T with its third component larger than zero. Therefore, the thrust vector T must be devised to achieve both tracking objective $(\tilde{x},\ \tilde{v}) \to 0_{6\times 1}$ and ensuring $\|T\| \neq 0$. In addition, since R_d is a function of (T, ψ_d), $\dot{R}_d$ depends on $(T, \dot{T}, \psi_d, \dot{\psi}_d)$. By (11) the desired angular velocity $\omega_d^\wedge = R_d^T \dot{R}_d$ and its first time derivative are given by

$$\omega_d(T, \dot{T}, \psi_d, \dot{\psi}_d) = \left(R_d^T \dot{R}_d\right)^\vee, \tag{12}$$

$$\dot{\omega}_d(T, \dot{T}, \ddot{T}, \psi_d, \dot{\psi}_d, \ddot{\psi}_d) = \left(R_d^T \ddot{R}_d + \dot{R}_d^T \dot{R}_d\right)^\vee. \tag{13}$$

Therefore, the thrust vector must be designed with sufficient smoothness to ensure $T \in \mathcal{C}^2$.

Notice that $f(R - R_d)e_z$ in (10) is a nonlinear coupling term that reflects the misalignment between the desired thrust direction R_de_z and the actual direction Re_z. It represents a bounded disturbance for the position control system (9)-(10), which vanishes as $R \to R_d$.

IV. Tracking Controller Design

A. Positioning Controller Design

The position control is aimed at designing a control law for the thrust vector $T \in \mathbb{R}^3$ that satisfies $\|T\| \neq 0$ to asymptotically stabilize the equilibrium $(\tilde{x}, \tilde{v}) = (0_{3\times 1}, 0_{3\times 1})$ by applying the thrust force $f = \|T\|$. The control law is first designed in this subsection ignoring the coupling term $f(R - R_d)e_z$ in (9)-(10) and the external disturbance f_d, which are then addressed together a bounded disturbance.

Motivated by [25], the following control law is proposed

$$T = mge_z + m\ddot{x}_d + (kI_3 + m(k_xI_3 + K_f))\,\mathrm{Tanh}(e_f), \tag{14}$$

$$\dot{e}_f = \mathrm{Cosh}^2(e_f)\Big(- K_f\mathrm{Tanh}(e_f) + k_x^2\big(1 - \frac{1}{m}\big)\tilde{x} - k\eta\Big) \tag{15}$$

$$\eta = \tilde{v} + k_x\tilde{x} + \mathrm{Tanh}(e_f), \tag{16}$$

with initial condition $e_f(0) = 0_{3\times 1}$, where $k > 0$ and $k_x > 0$ are scalar gains, $0 < K_f = K_f^T \in \mathbb{R}^{3\times 3}$ a diagonal matrix, and the hyperbolic functions are given by

$$\mathrm{Tanh}(u) = [\tanh(u_1), \tanh(u_2), \tanh(u_3)]^T \in \mathbb{R}^3,$$
$$\mathrm{Cosh}(u) = \mathrm{diag}\{\cosh(u_1), \cosh(u_2), \cosh(u_3)\} \in \mathbb{R}^{3\times 3},$$
$$\mathrm{Sech}(u) = \mathrm{diag}\{\mathrm{sech}(u_1), \mathrm{sech}(u_2), \mathrm{sech}(u_3)\} \in \mathbb{R}^{3\times 3},$$

for $u = [u_1, u_2, u_3]^T \in \mathbb{R}^3$.

Assuming that $\|\ddot{x}_d\| \leq \mu_d < g$, which is a realistic operating condition for most quadrotors, then by selecting controller gains satisfying the following

$$\frac{k}{m} + k_x + \lambda_{\max}(K_f) < g - \mu_d, \tag{17}$$

ensures the third component of thrust vector T to be greater than zero because the term mge_z is different from zero only in its third component. Therefore, $\|T\| \neq 0$ for all $t \geq 0$ in (14). Moreover, condition (17) also guarantees R_d in (11) to satisfy $R_d \in SO(3)$, $\forall t \geq 0$.

Stability of the equilibrium $(\tilde{x}, \tilde{v}) = 0_{6\times 1}$ under the control law (14) is stated in the following theorem.

*Theorem 4.1 (***Stability of positioning controller** (14)**):* Choose the gains as $0 < k_x < g - \mu_d$, $k > k_x$, and

$$\lambda_{\min}(K_f) > \frac{k_x}{4m^2}, \tag{18}$$

for the thrust control law (14)-(16), and set the thrust force $f = \|T\|$. Then the controller (14)-(16) globally exponentially stabilizes the equilibrium $(\tilde{x}, \tilde{v}) = 0_{6\times 1}$ of the translational error dynamics (9)-(10) under the assumption that the coupling term $f(R - R_d)e_z = 0_{3\times 1}$.

Proof: The proof starts by calculating error dynamics in the translational system. By (9) and (16), it has

$$\dot{\tilde{x}} = \tilde{v} = \eta - k_x\tilde{x} - \mathrm{Tanh}(e_f). \tag{19}$$

The dynamics of $\mathrm{Tanh}(e_f)$ can be calculated using $\frac{d}{dt}\mathrm{Tanh}(e_f) = \mathrm{Sech}^2(e_f)\dot{e}_f$ and (15) as

$$\frac{d}{dt}\mathrm{Tanh}(e_f) = -K_f\mathrm{Tanh}(e_f) + k_x^2\left(1 - \frac{1}{m}\right)\tilde{x} - k\eta. \tag{20}$$

At last, by taking time derivative of (16) and substituting (10), (19) and (20), yields

$$\begin{aligned} m\dot{\eta} &= m\dot{\tilde{v}} + mk_x\tilde{v} + m\mathrm{Sech}^2(e_f)\dot{e}_f \\ &= -mge_z - m\ddot{x}_d + fR_de_z \\ &\quad + mk_x\left(\eta - k_x\tilde{x} - \mathrm{Tanh}(e_f)\right) \\ &\quad + m\left(-K_f\mathrm{Tanh}(e_f) + k_x^2\left(1 - \frac{1}{m}\right)\tilde{x} - k\eta\right), \end{aligned}$$

where the coupling term $f(R-R_d)e_z$ in (10) is ignored. Adding the control law (14) in this last equation and in view of $fR_de_z = T$ results in

$$m\dot{\eta} = -m\,(k-k_x)\,\eta + k\mathrm{Tanh}(e_f) - k_x^2\tilde{x}. \tag{21}$$

The dynamics of the state $\zeta_1 := \left[\eta^T\ \tilde{x}^T\ \mathrm{Tanh}^T(e_f)\right]^T \in \mathbb{R}^9$ of the translational system in closed-loop with the controller (14)-(16) is given then by (19)-(21), which has the origin $\zeta_1 = 0_{9\times 1}$ as the unique equilibrium. To study its stability, consider the following positive definite function

$$V_1(\zeta_1) := \frac{m}{2}\|\eta\|^2 + \frac{k_x^2}{2}\|\tilde{x}\|^2 + \frac{1}{2}\|\mathrm{Tanh}(e_f)\|^2, \tag{22}$$

which is radially unbounded for all $\zeta_1 \in \mathbb{R}^9$ and satisfies

$$\begin{aligned} \varphi_1\|\zeta_1\|^2 \le & V_1(\zeta_1) \le \varphi_2\|\zeta_1\|^2, \\ \varphi_1 := \min\left\{\frac{m}{2}, \frac{k_x^2}{2}, \frac{1}{2}\right\}, & \quad \varphi_2 := \max\left\{\frac{m}{2}, \frac{k_x^2}{2}, \frac{1}{2}\right\}. \end{aligned} \tag{23}$$

The time evolution of (22) along the error dynamics (19)-(21) is given by

$$\begin{aligned} \dot{V}_1 &= m\eta^T\dot{\eta} + k_x^2\tilde{x}^T\dot{\tilde{x}} + \mathrm{Tanh}^T(e_f)\frac{d}{dt}\mathrm{Tanh}(e_f) \\ &= \eta^T\left(-m\,(k-k_x)\,\eta + k\mathrm{Tanh}(e_f) - k_x^2\tilde{x}\right) \\ &\quad + k_x^2\tilde{x}^T\left(\eta - k_x\tilde{x} - \mathrm{Tanh}(e_f)\right) \\ &\quad + \mathrm{Tanh}^T(e_f)\left(-K_f\mathrm{Tanh}(e_f) + k_x^2\left(1-\frac{1}{m}\right)\tilde{x} - k\eta\right) \\ &= -m\,(k-k_x)\,\eta^T\eta - k_x^3\tilde{x}^T\tilde{x} - \mathrm{Tanh}^T(e_f)K_f\mathrm{Tanh}(e_f) \\ &\quad - \frac{k_x^2}{m}\mathrm{Tanh}^T(e_f)\tilde{x} \\ &= -\zeta_1^TQ_1\zeta_1 \le -\lambda_{\min}(Q_1)\|\zeta_1\|^2 \le -\frac{\lambda_{\min}(Q_1)}{\varphi_2}V_1, \end{aligned} \tag{24}$$

where

$$Q_1 = \begin{bmatrix} m(k-k_x)I_3 & 0_{3\times 3} & 0_{3\times 3} \\ 0_{3\times 3} & k_x^3I_3 & -\frac{k_x^2}{2m} \\ 0_{3\times 3} & -\frac{k_x^2}{2m} & K_f \end{bmatrix} \in \mathbb{R}^{9\times 9}, \tag{25}$$

which is positive definite under conditions stated in the theorem resulting $\dot{V}_1$ negative definite. By invoking Theorem 4.10 of [26], the equilibrium $\zeta_1 = 0_{9\times 1}$ is globally exponentially stable. □

Taking into account the coupling term $f(R-R_d)e_z$ in (10), which is bounded by item 4) of Lemma 4.4, disturbance $\bar{f}_d := \left[fe_z^T(R-R_d)^T + f_d^T,\ 0_{1\times 3},\ 0_{1\times 3}\right]^T$ is bounded, resulting the closed-loop system error dynamics (19)-(21) in the following form

$$\dot{\zeta}_1 = A_1\zeta_1 + \bar{f}_d = \mathbf{f}_1(\zeta_1, \bar{f}_d), \tag{26}$$

$$A_1 = \begin{bmatrix} -m(k-k_x)I_3 & -k_x^2I_3 & kI_3 \\ I_3 & -k_xI_3 & -I_3 \\ -kI_3 & k_x^2\left(1-\frac{1}{m}\right)I_3 & -K_f \end{bmatrix}. \tag{27}$$

The following proposition gives a robustness result of the controller (14)-(16) in the presence of $\bar{f}_d$

*Proposition 4.2 (***Robustness of positioning controller (14)***):* Assume $\|\bar{f}_d\|_\infty := \sup_{t\ge 0}\|\bar{f}_d\| < \mu_f$, for some $\mu_f > 0$. Then, the perturbed system (26) holds the following properties:

1) For all initial condition $\zeta_1(0) \in \mathbb{R}^9$ and $t \ge 0$, $\|\zeta_1(t)\|_\infty \le \varphi_\infty\|\bar{f}_d\|_\infty < h$, where
$$\varphi_\infty := \frac{\varphi_4}{\lambda_{\min}(Q_1)}l_d\sqrt{\frac{\varphi_2}{\varphi_1}},$$
and $\varphi_1, \varphi_2, > 0$ are given in (23), $l_d \ge \|A_1\|$ the Lipschitz constant, for all $\zeta_1 \in B_h$ for some $h > 0$.
2) For all $\|\zeta_1(0)\| < h/\rho$, with $\rho := \sqrt{\varphi_2/\varphi_1} \ge 1$, there exists finite $\tau_f \ge 0$ such that
$$\|\zeta_1(t)\| \le (1-\epsilon_z)\delta_\infty < h, \quad \forall t \ge \tau_f,$$
for all $\epsilon_z > 0$, with $\delta_\infty := \varphi_\infty\|\bar{f}_d\|_\infty$ and
$$\tau_f \le \frac{\varphi_2h^2}{\lambda_{\min}(Q_1)\delta_\infty^2\epsilon_z}.$$

Thus, the state $\zeta_1(t)$ converges to the ball B_{δ_∞}, in finite time, and remains in it.

Proof: Since the equilibrium $\zeta_1 = 0_{9\times 1}$ is exponentially stable with the Lyapunov function $V_1(\zeta_1)$ in (22), according to Theorem 4.1, which satisfies $\|\frac{\partial V_1(\zeta_1)}{\partial\zeta_1}\| \le \varphi_4\|\zeta_1\|$, with $\varphi_4 := \sqrt{\max\{(cm)^2, c^2k_x^4, c^2\}}$. Under the assumption $\|\bar{f}_d\|_\infty < \mu_f$, and by invoking Theorem 5.3.1 of [27], the perturbed system (26) satisfies the properties stated in the theorem. □

Proposition 4.2 implies that controller (14) in closed loop with system (1)-(2) guarantees the boundedness of state (x, v), and consequently $\dot{v}$ and $T, \dot{T}, \ddot{T}$ are all bounded. This fact ensures that ω_d and $\dot{\omega}_d$ defined in (12)-(13) remain bounded, which is instrumental for the attitude control.

Remark 4.3 (Linear velocity measurement.): The position controller (14) can be implemented without linear velocity measurement v as follows. Let $y := \mathrm{Tanh}(e_f)$, then $\frac{d}{dt}\mathrm{Tanh}(e_f)$ in (20) can be obtained similar to that of [25] as

$$y = p - k\tilde{x}, \tag{28}$$

$$\begin{aligned} \dot{p} = & -k\,(k_x\tilde{x} + p - k\tilde{x}) - K_f(p - k\tilde{x}) \\ & + k_x^2\left(1-\frac{1}{m}\right)\tilde{x}, \quad p(0) = k\tilde{x}(0). \end{aligned} \tag{29}$$

So $\mathrm{Tanh}(e_f)$ can be calculated using only position measurements $\tilde{x}$. This feature is useful for nonaggressive applications when a fast inner attitude control loop ensures $R \approx R_d$ [3] or position regulation [14] since in this case no desired angular velocity and thus no linear velocity is needed in controller implementation.

B. Attitude Controller Design

The position controller in the previous subsection admits any attitude controller that achieves convergence $R \to R_d$ and dominates the bounded disturbance $f(R-R_d)e_z$. In this section, the attitude controller is developed using vector and gyro measurements.

Define the desired direction by unit vectors as follows:

$$v_{d,i} = R_d^Tr_i, \quad i = 1, 2, \cdots, n. \tag{30}$$

Then under Assumption A1, fact $v_i \to v_{d,i}$, $i = 1, 2, \cdots, n$, ensures $R \to R_d$. Thus, the attitude control problem becomes a vector alignment problem. The vector alignment error can be measured by the following variables

$$\varepsilon(t) = \sum_{i=1}^{n} k_i \left(1 - v_i^T v_{d,i}\right), \tag{31}$$

$$z(t) = \sum_{i=1}^{n} k_i v_i^\wedge v_{d,i}, \tag{32}$$

where $k_i > 0$ are weights assigned to each sensor according to its confidence level. Variable $\varepsilon \in \mathbb{R}$ relates the inner product between the actual direction v_i and the desired direction $v_{d,i}$, and measures the deviation both in alignment and in steering, while variable $z \in \mathbb{R}^3$ obtained by the cross product measures only the misalignment. Note that $v_i = v_{d,i}$ yields $\varepsilon = 0$ and $z = 0_{3\times 1}$, while $v_i = -v_{d,i}$ gives $z = 0_{3\times 1}$ and $\varepsilon = 2\sum_{i=1}^{n} k_i$.

The following lemma relates these error variables and gives a upper bound on the term $R - R_d$, which are instrumental for the subsequent control designs.

*Lemma 4.4 (***Alignment error variables** $\varepsilon(t)$ **and** $z(t)$**):**

1) Define the attitude error $\tilde{R} := RR_d^T \in SO(3)$. Then $z = 0_{3\times 1}$ implies $\tilde{R} = I_3$ or $\tilde{R} = R_j := I_3 + 2(v_{w_j}^\wedge)^2$, for $j = 1, 2, 3$, where $v_{w_j} \in \mathcal{S}^2$ are unit eigenvectors of the symmetric positive definite matrix [24]

$$W := -\sum_{i=1}^{n} k_i (r_i^\wedge)^2, \tag{33}$$

with the associated eigenvalues ordered, without loss of generality, as $\lambda_{w,1} \geq \lambda_{w,2} \geq \lambda_{w,3}$.
2) Variable $\varepsilon(t)$ satisfies $0 \leq \varepsilon \leq 2\sum_{i=1}^{n} k_i$.
3) For any $\alpha_1 > 0$ there exists $\beta > 0$, such that

$$\alpha_1 \varepsilon \leq \frac{\beta}{2}\|z\|^2, \quad \forall t \geq 0, \tag{34}$$

$\forall \tilde{R} \in SO(3)\backslash\mathcal{B}_\epsilon$, where $\mathcal{B}_\epsilon := \mathcal{B}_{\epsilon,1} \cup \mathcal{B}_{\epsilon,2} \cup \mathcal{B}_{\epsilon,3}$ with

$$\begin{aligned} \mathcal{B}_{\epsilon,j} &:= \left\{ \tilde{R} \in SO(3) \mid \tilde{R} = R_{\sigma,j},\ \forall \sigma \in [0, \epsilon] \right\}, \\ R_{\sigma,j} &:= I_3 - 2\sigma\sqrt{1-\sigma^2} v_{w_j}^\wedge + 2\left(1 - \sigma^2\right)(v_{w_j}^\wedge)^2, \end{aligned} \tag{35}$$

are closed balls centered at $R_j \in SO(3)$, and (arbitrarily small) radius $\epsilon_j > 0$, for $j = 1, 2, 3$. Furthermore, the constant β is given by

$$\beta \geq 2\frac{\lambda_{w,1}}{\epsilon_j^2 \lambda_{w,3}^2}\alpha_1,\ \forall j = 1, 2, 3. \tag{36}$$

4) Let $\bar{W} \in \mathbb{R}^{3\times 3}$ be defined as

$$\bar{W} := \sum_{i=1}^{n} k_i r_i r_i^T, \tag{37}$$

which is positive definite under Assumption A1 (Lemma 2, [24]). Let $\varpi := \mathrm{tr}\left(\bar{W}^{-1}\right) > 0$, then the following condition holds for all $\tilde{R} \in SO(3)\backslash\mathcal{B}_\epsilon$

$$\|R - R_d\| \leq \sqrt{\frac{\varpi\beta}{\alpha_1}}\|z\|, \quad \forall t \geq 0. \tag{38}$$

Proof: The proof of items (1)-(3) can be found in [23]. The proof of item (4) is provided in Appendix A. □

In addition, by (3) and the desired attitude trajectory $\dot{R}_d = R_d(\omega_d)^\wedge$, it results that $\dot{v}_i = v_i^\wedge \omega$ and $\dot{v}_{d,i} = v_{d,i}^\wedge \omega_d$. This in turn gives the dynamics of the alignment error variables (31)-(32) as follows

$$\dot{\varepsilon} = z^T(\omega - \omega_d), \tag{39}$$

$$\dot{z} = J(\omega - \omega_d) + z^\wedge \omega_d, \tag{40}$$

where $J \in \mathbb{R}^{3\times 3}$ is

$$J := \sum_{i=1}^{n} k_i \left(v_{d,i}^\wedge\right)^T v_i^\wedge, \tag{41}$$

and is bounded by $\|J\| \leq \sum_{i=1}^{n} k_i$.

Therefore, in view of item (1) of Lemma 4.4, the alignment error dynamics (39)-(40) has a desired equilibrium $(\tilde{R}, \omega - \omega_d) = (I_3, 0_{3\times 1})$ and three undesired equilibria $(\tilde{R}, \omega - \omega_d) = (R_j, 0_{3\times 1})$, for $j = 1, 2, 3$. The attitude control objective is then stated as designing a torque control law τ to achieve the convergence $(z, \omega - \omega_d) \to (0_{3\times 1}, 0_{3\times 1})$ and leaving unstable the three undesired equilibria $(\tilde{R}, \omega - \omega_d) = (R_j, 0_{3\times 1})$, i.e., the almost global stability of the desired equilibrium $(\tilde{R}, \omega - \omega_d) = (I_3, 0_{3\times 1})$.

Given a desired attitude trajectory $(R_d,\ \omega_d) \in SO(3) \times so(3)$ with $(\omega_d, \dot{\omega}_d)$ continuous and bounded, the following attitude controller is proposed

$$\tau = M\dot{\hat{\omega}}_r - (M\hat{\omega})^\wedge \omega_r - K_c\left(\hat{\omega} - \omega_r\right) - \left(\alpha_1 I_3 + \alpha_2 J^T\right) z, \tag{42}$$

$$\dot{\hat{\omega}}_r = -\lambda_c J\left(\hat{\omega} - \omega_d\right) - \lambda_c z^\wedge \omega_d + \dot{\omega}_d, \tag{43}$$

$$\omega_r = -\lambda_c z + \omega_d, \tag{44}$$

where $\lambda_c > 0$, $\alpha_{1,2} > 0$ and $0 < K_c \in \mathbb{R}^{3\times 3}$ are controller gains. The angular velocity estimate $\hat{\omega} := \omega_g - \hat{b}$ is obtained by correcting the gyro bias b in the measured gyro rate ω_g by the following gyro-bias observer

$$\hat{b} = \bar{b} - \sum_{i=1}^{n} k_i (v_{f,i}^\wedge)^T \Lambda_i v_i, \tag{45}$$

$$\dot{\bar{b}} = K_f \hat{\omega} + \gamma_f \sum_{i=1}^{n} k_i (\Lambda_i v_i)^\wedge (v_i - v_{f,i}), \tag{46}$$

$$\dot{v}_{f,i} = \gamma_f (v_i - v_{f,i}), \quad v_{f,i}(0) = v_i(0), \tag{47}$$

where $\hat{b} \in \mathbb{R}^3$ is the gyro bias estimate, $0 < \Lambda_i = \Lambda_i^T \in \mathbb{R}^{3\times 3}$, $i = 1, 2, ..., n$, are observer gains, $\gamma_f > 0$ is filter gain, and $K_f \in \mathbb{R}^{3\times 3}$ is defined as

$$K_f = \sum_{i=1}^{n} k_i (v_{f,i}^\wedge)^T \Lambda_i v_i^\wedge. \tag{48}$$

It was shown in [28] (Lemma 3.1) that $\|v_i - v_{f,i}\| < \epsilon_v$ for any $\epsilon_v > 0$ provided that the filter gain is large enough.

Let $\tilde{\omega} := \omega - \omega_r$, $\tilde{b} := \hat{b} - b$, and recall $\tilde{R}$ and R_j defined in item (1) of Lemma 4.4, the following theorem studies the equilibria of the rotational error dynamics.

*Theorem 4.5 (***Stability of attitude controller** (42)**):** Choose the controller gains $K_c = K_c^T > 0$, $\lambda_c > 0$, $\alpha_{1,2} > 0$, and the

gains in the observer $\gamma_f > 0$, $k_i > 0$, and $\Lambda_i = \Lambda_i^T > 0$, for $i = 1, 2, \ldots, n$ such that

$$\lambda_o := \lambda_{\min}(K_o) - \epsilon_v \sum_{i=1}^{n} k_i \lambda_{\max}(\Lambda_i) > \frac{\|G\|^2}{4\lambda_{\min}(K_c)}, \quad (49)$$

$$\lambda_a := \alpha_1 - \alpha_2 \sum_{i=1}^{n} k_i > 0, \quad (50)$$

where

$$K_o := \sum_{i=1}^{n} k_i (v_i^\wedge)^T \Lambda_i v_i^\wedge, \quad (51)$$

$$G := K_c - \omega_r^\wedge M + \lambda_c M J. \quad (52)$$

Then in the absence of external disturbances, the controller (42)-(44) with the bias observer (45)-(47) in closed-loop with the rotational dynamics (3)-(4) holds, for $j = 1, 2, 3$, the following properties

1) The set of equilibria is given by $\{(\tilde{R}, \tilde{\omega}, \tilde{b}) \in SO(3) \times \mathbb{R}^3 \times \mathbb{R}^3 \mid (I_3, 0_{3\times1}, 0_{3\times1}),\ (R_j, 0_{3\times1}, 0_{3\times1})\}$.
2) Equilibrium $(\tilde{R}, \tilde{\omega}, \tilde{b}) = (I_3, 0_{3\times1}, 0_{3\times1})$ is almost globally asymptotically stable for all $(\tilde{R}(0), \tilde{\omega}(0), \tilde{b}(0)) \in \mathcal{X}_a := SO(3)\backslash\{R_j\} \times \mathbb{R}^3 \times \mathbb{R}^3$ and almost semiglobally exponentially stable for $(\tilde{R}(0), \tilde{\omega}(0), \tilde{b}(0)) \in \mathcal{X}_e := SO(3)\backslash\mathcal{B}_\epsilon \times \mathbb{R}^3 \times \mathbb{R}^3$, where $\mathcal{B}_\epsilon$ is the union of closed balls given by (35) defined in item (3) of Lemma 4.4, which are centered at R_j with arbitrary small radius $\epsilon_j > 0$.
3) The undesired equilibria $(\tilde{R}, \tilde{\omega}, \tilde{b}) = (R_j, 0_{3\times1}, 0_{3\times1})$ are unstable.

Proof: A similar proof can be found in [23] using quaternion representation of the attitude. For clarity, proof of item 1) and 2) of the present theorem are given here.

By (45)-(47) the dynamics of the bias estimation error is

$$\dot{\tilde{b}} = \dot{\hat{b}} - \dot{b} = -K_f \tilde{b}. \quad (53)$$

Taking the time derivative of $\tilde{\omega} = \omega - \omega_r$ and substituting (4) in closed-loop with controller (42)-(44), yields

$$M\dot{\tilde{\omega}} = (M\omega)^\wedge \tilde{\omega} - K_c \tilde{\omega} + G\tilde{b} - \left(\alpha_1 I_3 + \alpha_2 J^T\right) z. \quad (54)$$

The dynamics (39) and (40) are rewritten by adding and subtracting ω_r in ω as follows

$$\dot{z} = J\tilde{\omega} - \lambda_c J z + z^\wedge \omega_d, \quad (55)$$

$$\dot{\varepsilon} = z^T \tilde{\omega} - \lambda_c z^T z. \quad (56)$$

Let $\zeta_2 := \left[z^T, \tilde{\omega}^T, \tilde{b}^T\right]^T \in \mathbb{R}^9$ be the state of the closed-loop system defined by (53)-(55). Therefore, the origin $\zeta_2 = 0_{9\times1}$ is the unique equilibrium of the error dynamics. Since $z = 0_{3\times1}$ implies that $\tilde{R} = I_3$ or $\tilde{R} = R_j$ according to item (1) of Lemma 4.4, the set of equilibria is given in the item (1) of the present theorem.

To prove the stability of the desired equilibrium where $\tilde{R} = I_3$, consider the following positive definite function

$$V_2(\zeta_2, t) := \frac{1}{2}\tilde{\omega}^T M \tilde{\omega} + \frac{1}{2}\|\tilde{b}\|^2 + \frac{\alpha_2}{2}\|z\|^2 + \alpha_1 \varepsilon(t), \quad (57)$$

which is positive definite and radially unbounded for all $\left(\tilde{R}, \tilde{\omega}, \tilde{b}\right) \in \mathcal{X}_a$. In addition, $V_2(\zeta_2, t)$ satisfies

$$V_2 \geq \min\left\{\frac{1}{2}\lambda_{\min}(M), \frac{1}{2}, \frac{\alpha_2}{2}\right\}\|\zeta_2\|^2. \quad (58)$$

By (56) the time derivative of (57) along the closed loop trajectories (53)-(55) is

$$\begin{aligned}\dot{V}_2 &= \tilde{\omega}^T M \dot{\tilde{\omega}} + \tilde{b}^T \dot{\tilde{b}} + \alpha_2 z^T \dot{z} + \alpha_1 \dot{\varepsilon} \\ &= -\tilde{\omega}^T K_c \tilde{\omega} + \tilde{\omega}^T G \tilde{b} - \tilde{b}^T K_f \tilde{b} - \lambda_c z^T \left(\alpha_1 I_3 + \alpha_2 J\right) z \\ &\leq -\lambda_{\min}(Q_2)\|\zeta_2\|^2, \end{aligned} \quad (59)$$

where $Q_2 \in \mathbb{R}^{3\times3}$ is calculated as

$$Q_2 = \begin{bmatrix} \lambda_c \lambda_a & 0 & 0 \\ 0 & \lambda_{\min}(K_c) & -\frac{1}{2}\|G\| \\ 0 & -\frac{1}{2}\|G\| & \lambda_o \end{bmatrix}. \quad (60)$$

Therefore, (59) is negative definite satisfying conditions (49)-(50), because matrix G in (52) is bounded for any bounded ω_d. Consequently, equilibrium $\zeta_2 = 0_{9\times1}$ is asymptotically stable. By item (1) of Lemma 4.4, convergence $z \to 0_{3\times1}$ implies that $\tilde{R} \to I_3$ or $\tilde{R} = R_j$, $j = 1, 2, 3$. Thus, only almost global stability can be achieved by excluding the undesired equilibria R_j from $SO(3)$. Therefore, equilibrium $(\tilde{R}, \tilde{\omega}, \tilde{b}) = (I_3, 0_{3\times1}, 0_{3\times1})$ is almost globally asymptotically stable.

Moreover, by item (3) of Lemma 4.4 $\forall(\tilde{R}, \tilde{\omega}, \tilde{b}) \in \mathcal{X}_e$ function V_2 satisfies

$$V_2 \leq \max\left\{\frac{1}{2}\lambda_{\max}(M), \frac{1}{2}, \frac{\alpha_2 + \beta}{2}\right\}\|\zeta_2\|^2, \quad (61)$$

where β verifies (36). Therefore, the time derivative (59) fulfills

$$\dot{V}_2 \leq -\lambda_{\min}(Q_2)\|\zeta_2\|^2 \leq -\frac{\lambda_{\min}(Q_2)}{\max\left\{\frac{1}{2}\lambda_{\max}(M), \frac{1}{2}, \frac{\alpha_2+\beta}{2}\right\}} V_2.$$

This results in a exponentially decaying of V_2 by given (58), showing that the equilibrium $\zeta_2 = 0_{9\times1}$ is globally exponentially stable. Using the same arguments as in the almost global asymptotic stability of the equilibrium $(\tilde{R}, \tilde{\omega}, \tilde{b})$ above, and noting that that in the closed-loop system (53)-(55) the parameter β in (36) can be increased to cover almost the entire state space except for trajectories that start in $(\tilde{R}(0), \tilde{\omega}(0), \tilde{b}(0)) = (R_j, 0_{3\times1}, 0_{3\times1})$, which has Lebesgue measure zero, the semiglobal exponential stability of the desired equilibrium follows [12]. □

C. Main Result

This section gives the main result of this work. Position tracking is first stated without external disturbances in (1)-(4), then it is shown the resulting controller is robust in the presence of the external disturbances.

*Theorem 4.6 (***Tracking control):** Consider the position controller $f = \|T\|$ with the thrust vector T in (14) and the attitude controller (42) with the gyro-bias estimation (45) in closed loop with the system (1)-(4). Choose the design parameters for

- position controller: $K_f = K_f^T > 0$, and $k > k_x > 0$,

- attitude controller: $K_c = K_c^T > 0$, $\lambda_c > 0$, and $\alpha_1, \alpha_2 > 0$,
- gyro-bias observer: $\gamma_f > 0$, $k_i > 0$, and $\Lambda_i = \Lambda_i^T > 0$, for $i = 1, 2, \ldots, n$,

such that conditions (17)-(18), and (49)-(50) are satisfied. Then, the equilibrium $(\zeta_1, \tilde{R}, \tilde{\omega}, \tilde{b}) = (0_{9\times1}, I_3, 0_{3\times1}, 0_{3\times1})$ is semiglobally exponentially stable for all $(\zeta_1(0), \tilde{R}(0), \tilde{\omega}(0), \tilde{b}(0)) \in \mathcal{X}_e' := \mathbb{R}^9 \times SO(3)\backslash\mathcal{B}_\epsilon \times \mathbb{R}^3 \times \mathbb{R}^3$.

Proof: The error dynamics of η (21) including the coupling term $f(R - R_d)e_z$ is given by

$$m\dot{\eta} = -m\,(k - k_x)\,\eta + k\mathrm{Tanh}(e_f) - k_x^2\tilde{x} + f(R - R_d)e_z. \tag{62}$$

Therefore, the error state $\zeta_3 := \left[\zeta_1^T, \zeta_2^T\right]^T \in \mathbb{R}^{18}$ of the overall system (19)-(20), (53)-(55), and (62) has $(\zeta_1, \tilde{R}, \tilde{\omega}, \tilde{b}) = (0_{9\times1}, I_3, 0_{3\times1}, 0_{3\times1})$ the unique equilibrium. This is because in the presence of coupling term $f(R - R_d)e_z \neq 0_{3\times1}$ in (62) the three undesired equilibria $(\zeta_1, \tilde{R}, \tilde{\omega}, \tilde{b}) = (0_{9\times1}, R_j, 0_{3\times1}, 0_{3\times1})$ are no longer equilibria of the overall closed-loop dynamics. To study the stability of the equilibrium consider the following positive definite and radially unbounded function for all $\zeta_3 \in \mathbb{R}^{18}$

$$V_3(\zeta_3, t) := cV_1(\zeta_1) + V_2(\zeta_2, t), \tag{63}$$

where V_1 and V_2 are given in (22) and (57), respectively, and $c > 0$ is a positive constant. By (23), (58) and (61) function (63) satisfies $\forall(\zeta_1, \tilde{R}, \tilde{\omega}, \tilde{b}) \in \mathcal{X}_e'$ that

$$\gamma_1\|\zeta_3\|^2 \leq V_3(\zeta_3, t) \leq \gamma_2\|\zeta_3\|^2, \tag{64}$$

where

$$\gamma_1 := \min\left\{\frac{cm}{2}, \frac{ck_x^2}{2}, \frac{c}{2}, \frac{\lambda_{\min}(M)}{2}, \frac{1}{2}, \frac{\alpha_2}{2}\right\},$$
$$\gamma_2 := \max\left\{\frac{cm}{2}, \frac{ck_x^2}{2}, \frac{c}{2}, \frac{\lambda_{\max}(M)}{2}, \frac{1}{2}, \frac{\alpha_2 + \beta}{2}\right\}.$$

By (24) and (59) and taking the time derivative of (63), yields

$$\begin{aligned}
\dot{V}_3 &= -cm\,(k - k_x)\,\eta^T\eta + cf\eta^T(R - R_d)e_z - ck_x^3\tilde{x}^T\tilde{x} \\
&\quad - c\mathrm{Tanh}^T(e_f)K_f\mathrm{Tanh}(e_f) - c\frac{k_x^2}{m}\mathrm{Tanh}^T(e_f)\tilde{x} \\
&\quad - \tilde{\omega}^T K_c\tilde{\omega} + \tilde{\omega}^T G\tilde{b} - \tilde{b}^T K_f\tilde{b} - \lambda_c z^T\,(\alpha_1 I_3 + \alpha_2 J)\,z \\
&\leq -cm\,(k - k_x)\,\|\eta\|^2 + cf\|R - R_d\|\|\eta\| - ck_x^3\|\tilde{x}\|^2 \\
&\quad - c\lambda_{\min}(K_f)\|\mathrm{Tanh}(e_f)\|^2 + c\frac{k_x^2}{m}\|\mathrm{Tanh}(e_f)\|\|\tilde{x}\| \\
&\quad - \lambda_{\min}(K_c)\|\tilde{\omega}\|^2 + \|G\|\|\tilde{\omega}\|\|\tilde{b}\| - \lambda_o\|\tilde{b}\|^2 - \lambda_c\lambda_a\|z\|^2
\end{aligned}$$

In view of condition (72) of item 4) in Lemma 4.4 item (4), it has

$$\begin{aligned}
\dot{V}_3 &\leq -\lambda_{\min}(Q_3)\left(\|z\|^2 + \|\eta\|^2\right) - \lambda_{\min}(Q_4)\left(\|\tilde{\omega}\|^2 + \|\tilde{b}\|^2\right) \\
&\quad - \lambda_{\min}(Q_5)\left(\|\tilde{x}\|^2 + \|\mathrm{Tanh}(e_f)\|^2\right),
\end{aligned}$$

where

$$Q_3 = \begin{bmatrix} \lambda_c\lambda_a & -c\frac{f}{2}\sqrt{\frac{\varpi\beta}{\alpha_1}} \\ -c\frac{f}{2}\sqrt{\frac{\varpi\beta}{\alpha_1}} & cm\,(k - k_x) \end{bmatrix},$$
$$Q_4 = \begin{bmatrix} \lambda_{\min}(K_c) & -\frac{1}{2}\|G\| \\ -\frac{1}{2}\|G\| & \lambda_o \end{bmatrix},$$
$$Q_5 = \begin{bmatrix} ck_x^3 & -c\frac{k_x^2}{2m} \\ -c\frac{k_x^2}{2m} & c\lambda_{\min}(K_f) \end{bmatrix}.$$

Thus,

$$\dot{V}_3 \leq -\gamma_3\|\zeta_3\|^2 \leq -\frac{\gamma_3}{\gamma_2}V_3, \tag{65}$$

with γ_3 given by

$$\gamma_3 := \min\left\{\lambda_{\min}(Q_3), \lambda_{\min}(Q_4), \lambda_{\min}(Q_5)\right\} \tag{66}$$

Note that matrices Q_5 and Q_4 are positive definite under conditions (18) and (49), and matrix Q_3 is positive definite under condition (50) provided that $k > k_x$, for any constant c that satisfies

$$0 < c < \frac{\alpha_1\lambda_c\lambda_a\,(k - k_x)}{mg^2\varpi\beta},$$

given that $f < 2mg$ by condition (17). Therefore $\dot{V}_3$ is negative definite for some $\gamma_3 > 0$ in (65), resulting $V_3 \to 0$ exponentially from any initial condition $(\zeta_1(0), \tilde{R}(0), \tilde{\omega}(0), \tilde{b}(0)) \in \mathcal{X}_e'$. Since the domain of attraction $\mathcal{X}_e'$ can be made arbitrarily large to cover almost the whole state space by choosing properly the design parameter such that $SO(3)\backslash\mathcal{B}_\epsilon$ covers almost the entire group $SO(3)$, semi-global exponential stability of equilibrium $(\zeta_1, \tilde{R}, \tilde{\omega}, \tilde{b}) = (0_{9\times1}, I_3, 0_{3\times1}, 0_{3\times1})$ is concluded. □

In the presence of the disturbances, the following proposition ensures the robustness of the proposed tracking controller.

*Proposition 4.7 (***Robustness of the tracking controller):** Assume that the disturbances $u_d := \left[f_d^T,\ 0_{1\times3},\ 0_{1\times3},\ 0_{1\times3},\ \tau_d^T,\ 0_{1\times3}\right]^T$ satisfies

- Assumption A3:

$$\|u_d\| \leq \delta_d < \frac{\gamma_3}{\gamma_4}\sqrt{\frac{\gamma_1}{\gamma_2}}\mu_u r,$$

for some $\mu_u < 1$, where $\gamma_1, \gamma_2 > 0$ are defined in (64), $\gamma_3 > 0$ is given in (66), and $\gamma_4 > 0$ is defined as

$$\gamma_4 := \sqrt{\max\left\{(cm)^2, c^2k_x^4, c^2, \lambda_{\max}^2(M), 1, \alpha_2^2\right\}}$$

being that $\|\frac{\partial V_3(\zeta_3,t)}{\partial\zeta_3}\| \leq \gamma_4\|\zeta_3\|$.

Then all variables are bounded and the error state $\zeta_3(t)$ of the overall system reaches the ball B_{r_d} in finite time and remains in it.

Proof: In the presence of the bounded external disturbances (f_d, τ_d) in the motion equations (1)-(4), the error dynamics of the overall system (19)-(20), (53)-(55), and (62) can be rewritten as

$$\dot{\zeta}_3 = F(t)\zeta_3 + u(t) + u_d = \mathbf{f}(\zeta_3, t, u_d), \tag{67}$$

where $u(t) := \left[f e_z^T (R - R_d)^T,\ 0_{1\times 15} \right]^T$, and

$$F(t) := \begin{bmatrix} A_1 & 0_{9\times 9} \\ 0_{9\times 9} & A_2(t) \end{bmatrix},$$

$$A_2(t) = \begin{bmatrix} -\lambda_c J - \omega_d^\wedge & J & 0_{3\times 3} \\ -M^{-1}\left(\alpha_1 I_3 + \alpha_2 J^T\right) & M^{-1}((M\omega)^\wedge - K_c) & M^{-1}G \\ 0_{3\times 3} & 0_{3\times 3} & -K_f \end{bmatrix}.$$

with $A_1 \in \mathbb{R}^{9\times 9}$ defined in (27).

Since the equilibrium $\zeta_3 = 0_{18\times 1}$ is exponentially stable of the nominal system $\dot{\zeta}_3 = \mathbf{f}(\zeta_3, t, 0_{18\times 1})$ with the Lyapunov function $V_3(\zeta_3, t)$ in view of Theorem 4.6 and $\|\frac{\partial V_3(\zeta_3,t)}{\partial \zeta_3}\| \leq \gamma_4 \|\zeta_3\|$, it follows from Lemma 9.2 of [26] that for all initial conditions $\|\zeta_3(t_0)\| \leq \sqrt{\gamma_1/\gamma_2} r$, the perturbed system (67) satisfies

$$\|\zeta_3(t)\| \leq \begin{cases} \sqrt{\frac{\gamma_2}{\gamma_1}} \|\zeta_3(t_0)\| \mathrm{e}^{-r_z(t-t_0)}, & \text{if} \quad t_0 \leq t < t_0 + \tau, \\ r_d, & \text{if} \quad t \geq t_0 + \tau, \end{cases} \tag{68}$$

for some finite $\tau > 0$, with $r_z := \frac{(1-\mu_u)\gamma_3}{2\gamma_2}$, $r_d := \frac{\gamma_4}{\gamma_3}\sqrt{\frac{\gamma_2}{\gamma_1}\frac{\delta_d}{\mu_u}}$. That is, $\zeta_3(t)$ reaches the ball B_{r_d} in finite time and remains in it. □

Remark 4.8 (Semiglobal exponential stability): In light of the bound on $\|R - R_d\|$ in item (4) of Lemma 4.4, semiglobal exponential stability of the equilibrium in Theorem 4.6 is achieved under the position controller $f = \|T\|$ with the thrust vector T in (14) and the attitude controller (42) compared with local exponential stability in [14]. Note that these controllers can be designed independently provided (1) the thrust force f in the position controller is bounded, and (2) the difference $\|R - R_d\|$ between the actual attitude R and the desired attitude R_d in the attitude controller goes zero. Both conditions are ensured by Theorem 4.5, Theorem 4.6, and item (4) of Lemma 4.4. This modular design brings several salient features, such as stability analysis and control parameter tuning.

Remark 4.9 (Adaptive attitude tracking): Thanks to modular design, adaptive techniques can be used to deal with the uncertainty in the inertia matrix M of rotational dynamics (4). For example, the adaptive controller (28) of [23] may be used in place of the attitude controller (42). In this case, under conditions stated in Theorem 4.8 of [23] almost global asymptotic stability instead of almost semiglobal exponential stability of the desired equilibrium in Theorem 4.6 can be proved.

Remark 4.10 (Practical issues): To implement the tracking controllers, the following practical issues may be taken into account.

- *Desired angular velocity*. The attitude controller (42) depends on the desired angular acceleration $\dot{\omega}_d$ through (43), which in turn requires the second time derivative of the thrust control (14) by (13), thus needs the acceleration error $\dot{\tilde{v}}$ for its implementation. To avoid using the acceleration $\dot{v}$ a filtered version of ω_d to approximate $\dot{\omega}_d$ as proposed [7] may be employed as in the following

$$\begin{aligned} \dot{\vartheta}_1 &= \vartheta_2, \\ \dot{\vartheta}_2 &= -2A\vartheta_2 - A^2(\vartheta_1 - \omega_d), \end{aligned} \tag{69}$$

  where $A \in \mathbb{R}^{3\times 3}$ is a diagonal positive definite matrix. Then, $\vartheta_2 \in \mathbb{R}^3$ is an approximation of $\dot{\omega}_d$. The boundedness of $\|\vartheta_2 - \dot{\omega}_d\|$ is ensured [7], which contributes a bounded disturbance $\tau_d = M(\vartheta_2 - \dot{\omega}_d)$ when using ϑ_2 instead of $\dot{\omega}_d$ in (43). The stability of the overall system is ensured by the robustness property in Proposition 4.7.
- *Vector measurements.* There are several ways to acquire vector measurements required for the attitude controller, such as using two magnetometers placed in the UAV with different orientation, a CCD camera, or an IMU with one magnetometer and one accelerameter. In this last case, the measured body acceleration $v_a = R^T r_a$, with r_a depending on the apparent acceleration $ge_z + \dot{v}$ which is not a known constant inertial reference vector. However, when $\|\dot{v}\| << g$, $r_a \approx e_z + \bar{r}_a$, where $\|\bar{r}_a\| << 1$, which can be considered as a bounded disturbance and tolerated by the robustness of the controller.

V. SIMULATIONS

To illustrate the main result (Theorem 4.6) numerical simulations were carried out. Four scenarios were considered. In Scenario 1 the vector, gyro rate, position and linear velocity measurements are noise free and the inertia matrix is known; In Scenario 2 the position, linear velocity, inertial vector, and angular velocity measurements are contaminated by noise, while the inertia matrix remains known; In Scenario 3 a $\pm 30\%$ uncertainty is added in the inertia matrix while the measurements are noise free, and In Scenario 4 the apparent acceleration is measured, and therefore the corresponding inertial reference is not constant as commented in Remark 4.10. In all scenarios, the parameters of the quadrotor were taken from the experimental UAV from [29], the initial conditions and the design parameters were the same and are shown in Table I. The desired trajectory was chosen as a Lemniscata calculated by $x_d(t) = [2.5\cos((2\pi/60)t), 3\sin((2\pi/60)t)\cos((2\pi/60)t), 3]^T$ (m). The desired angular acceleration $\dot{\omega}_d$ was approximated by the linear filter (69).

A. Scenario 1. Ideal situation.

Figure 2 shows the performance of the proposed controller in Scenario 1, where the attitude error $\frac{1}{2}\mathrm{tr}(I_3 - \tilde{R})$, the vector alignment error z, the angular velocity error $\tilde{\omega}$, the gyro-bias estimation error $\tilde{b}$, and the position error $\tilde{x}$ are shown. The composite error η and the auxiliary variable $\mathrm{Tanh}(e_f)$ in Figs. 2(f)-(g). Note that after about $5[s]$ transient they convergence to zero of as established in Theorem 4.6. The control thrust force f and the control torque τ are shown in Figs. 2(h) and (i), respectively. It is observed that the thrust force reaches a steady-state value of 4.6 (N) maintaining away from zero in all time, while the norm of torque control remains below 0.01 (Nm).

A 3D plot is given in Fig. 3 showing the actual path of the AUV and the desired one.

TABLE I
PARAMETERS AND INITIAL CONDITIONS, FOR $i = 1, 2, 3$.

Initial Condition	Value	Unit
$\omega(0)$	$0_{3\times1}$	(rad/s)
$R(0)$	I_3	
$x(0)$	$0_{3\times1}$	(m)
$v(0)$	$0_{3\times1}$	(m/s)
$\psi_d(0)$	$\pi/4$	(rad)
$\dot{\psi}_d(0)$	0	(rad/s)
$e_f(0)$	$0_{3\times1}$	
$\hat{b}(0)$	$0_{3\times1}$	
Parameter	**Value**	**Unit**
M	$\text{diag}\{8.28, 8.28, 15.7\} \times 10^{-3}$	Kgm^2
m	0.467	Kg
b	$[0.2, 0.1, -0.1]^T$	(rad/s)
Inertial Vectors		
r_1	$[0, 0, 1]^T$	
r_2	$(1/\sqrt{3})[1, 1, 1]^T$	
r_3	$r_1^\wedge r_2 / \|r_1^\wedge r_2\|$	
k_i	0.1	
Position Controller (14)		
k	4	
k_x	0.1	
K_f	I_3	
Attitude Controller (42)		
K_c	I_3	
λ_c	1	
α_1	1	
α_2	0.01	
Bias Observer (45)		
Λ_i	$10 I_3$	
γ_f	10000	
Filter (69)		
A	20	

B. Scenario 2. Noisy measurements.

The noisy measurements of x, v, ω_g, and v_i, for $i = 1, 2, 3$, were simulated as follows: $x_m = x + \nu_1 \varrho_1$, $v_m = v + \nu_2 \varrho_2$, $\omega_m = \omega_g + \nu_3 \varrho_3$, and $v_{m,i} = (v_i + \nu_4 \varrho_4)/\|v_i + \nu_4 \varrho_4\|$, where $\varrho_j \in \mathbb{R}^3$ are zero-mean Gauss distributions with unit variance, for all $j = 1, 2, 3, 4$, and $\nu_{1,2} \in N(0, 0.05)$, $\nu_{3,4} \in N(0, 0.1)$ are uniform distributions.

The attitude error in Fig. 4(a) shows no substantial changes compared to Scenario 1, while the norm of the alignment variable z remained oscillates inside of 0.025 (Fig. 4(b)), which is of the same magnitude of the noise density in the vector measurements $v_{m,i}$ given in Table I). Note that the angular velocity error $\tilde{\omega} = \omega - \omega_r = \omega + \lambda_c z - \omega_d$ in Fig. 4(c) is most affected by the noise because of the sum effect of noise in vector measurements $v_{m,i}$ through z, position x_m, the linear velocity v_m through $\omega_d(T, \dot{T}, \psi_d, \dot{\psi}_d)$ in (12). The norm of the gyro-bias estimation error $\tilde{b}$ in Fig. 4(d) remains below 0.2, which is due to the sum of the noise in the vector measurements $v_{m,i}$ and the gyro sensor ω_m. The noise in $\tilde{b}$ can be reduced by decreasing the observer gain Λ_i or increasing the filter gain γ_f, without affecting the performance of the overall system. Figs. 4(e)-(f) illustrate the norm of sate variables $\tilde{x}$, η, and $\text{Tanh}(e_f)$, all remained below 0.1, in accordance to the sum of the noise density in the position and speed measurements. The control thrust force f and the torque control τ in Figs. 4(h) and (i) remained bounded and close to the values in Scenario 1, as established in Proposition 4.7.

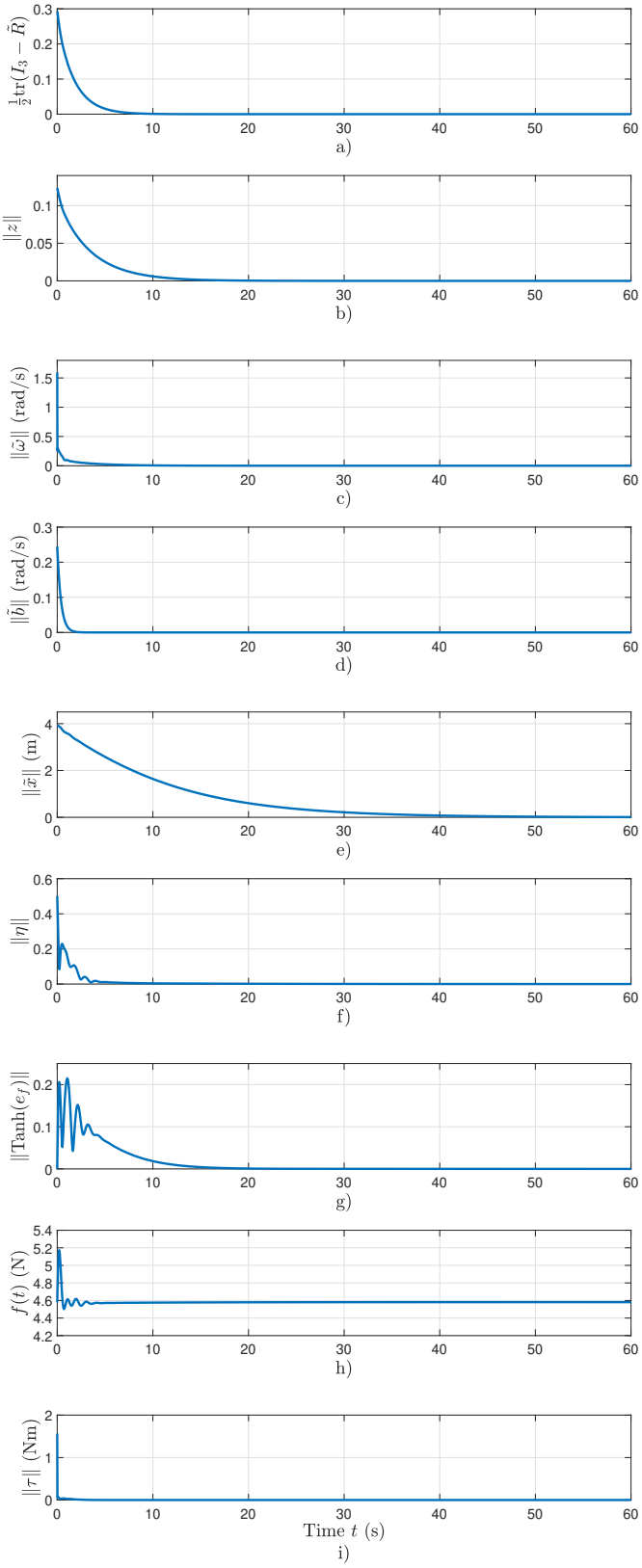

Fig. 2. Scenario 1 (ideal situation). Performance of the proposed controller under noise-free measurements and known inertia matrix.

C. Scenario 3. Parametric uncertainty.

A $\pm 30\%$ of uncertainty in the inertia matrix with noise-free measurements is considered for this scenario. Fig. 5

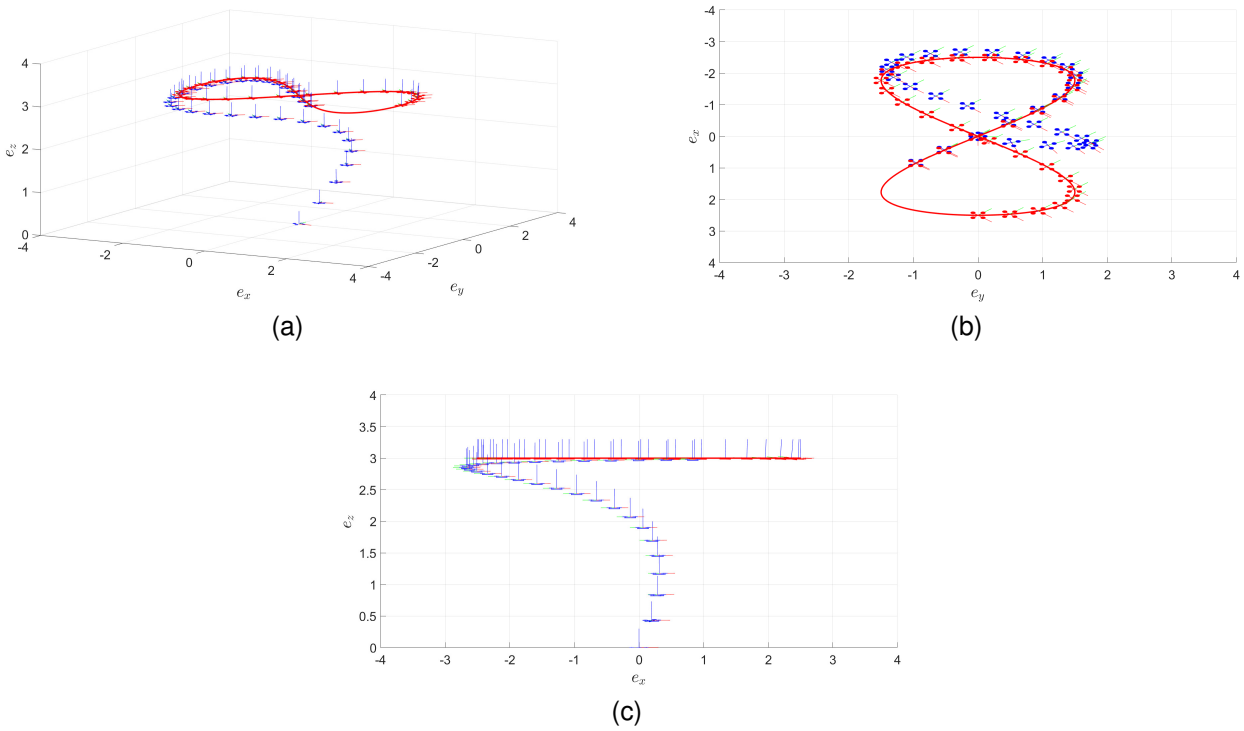

Fig. 3. Scenario 1 (ideal situation). The actual path of the quadrotor (blue) tracks the desired path (red). (a) A 3D view in the inertial frame $\{e_x, e_y, e_z\}$ [m]. (b) Plane $\{e_x - e_y\}$ view. (c) Plane $\{e_x - e_z\}$ view.

displays the simulation results. No significant changes in the performance are observed, with the convergence times of error state and the control efforts practically the same.

D. Scenario 4. Apparent acceleration.

The accelerameter is used to acquire one of the two vector measurements as commented in Remark 4.10 in this scenario, keeping all the conditions as in Scenario 1, except that the inertial reference vector r_1 in Table I was replaced by $(ge_z + \dot{v})/\|ge_z + \dot{v}\|$, i.e., the first vector measurement is $v_1 = R^T(ge_z + \dot{v})/\|ge_z + \dot{v}\|$. Fig. 6 illustrates the simulation results. As it can be observed, there are no substantial differences respect to the performance of controller in Scenario 1, except for a slight oscillation in the norm $\|\mathrm{Tanh}(e_f)\|$ after 20 (s).

VI. Conclusion

This paper has designed a tracking control for a quadrotor UAV by using position, linear velocity, angular velocity, and inertial vector measurements. No attitude representation nor its measurement in any form is needed to implement the controller. Semiglobal exponential stability of the overall closed-loop system was demonstrated. Numerical simulations were included to verify the theoretical results, illustrating the robustness of the proposed controller in the presence of measurement noise, inertia parametric uncertainty, and using the apparent acceleration as one of the vector measurements..

Appendix
Proof of Lemma 4.4 item (4)

Given n inertial vectors $v_i = R^T r_i$, and their corresponding desired vectors $v_{d,i} = R_d^T r_i$, where $r_i \in \mathcal{S}^2$ are constant inertial references for $i = 1, 2, \cdots, n$. The following matrices can be written

$$H_B = \left[\sqrt{k_1}v_1 \ \sqrt{k_2}v_2 \ \cdots \ \sqrt{k_n}v_n\right] \in \mathbb{R}^{3\times n},$$
$$H_D = \left[\sqrt{k_1}v_{d,1} \ \sqrt{k_2}v_{d,2} \ \cdots \ \sqrt{k_n}v_{d,n}\right] \in \mathbb{R}^{3\times n},$$
$$H_I = \left[\sqrt{k_1}r_1 \ \sqrt{k_2}r_2 \ \cdots \ \sqrt{k_n}r_n\right] \in \mathbb{R}^{3\times n},$$

then, it is held

$$\bar{W} = H_I H_I^T, \tag{70}$$
$$\begin{aligned}\varepsilon &= \sum_{i=1}^{n} k_i \left(1 - v_i^T v_{d,i}\right) = \frac{1}{2}\sum_{i=1}^{n} k_i \|v_i - v_{d_1}\|^2 \\ &= \frac{1}{2}\mathrm{tr}\left(\left(H_B - H_D\right)^T \left(H_B - H_D\right)\right).\end{aligned} \tag{71}$$

Furthermore, being $H_B - H_D = (R^T - R_d^T)H_I$, it can be solved for $R^T - R_d^T$, by using (70), as follows

$$\begin{aligned}\left(H_B - H_D\right) H_I^T &= (R^T - R_d^T)H_I H_I^T \\ &= (R^T - R_d^T)\bar{W}, \\ \left(H_B - H_D\right) H_I^T \bar{W}^{-1} &= R^T - R_d^T,\end{aligned} \tag{72}$$

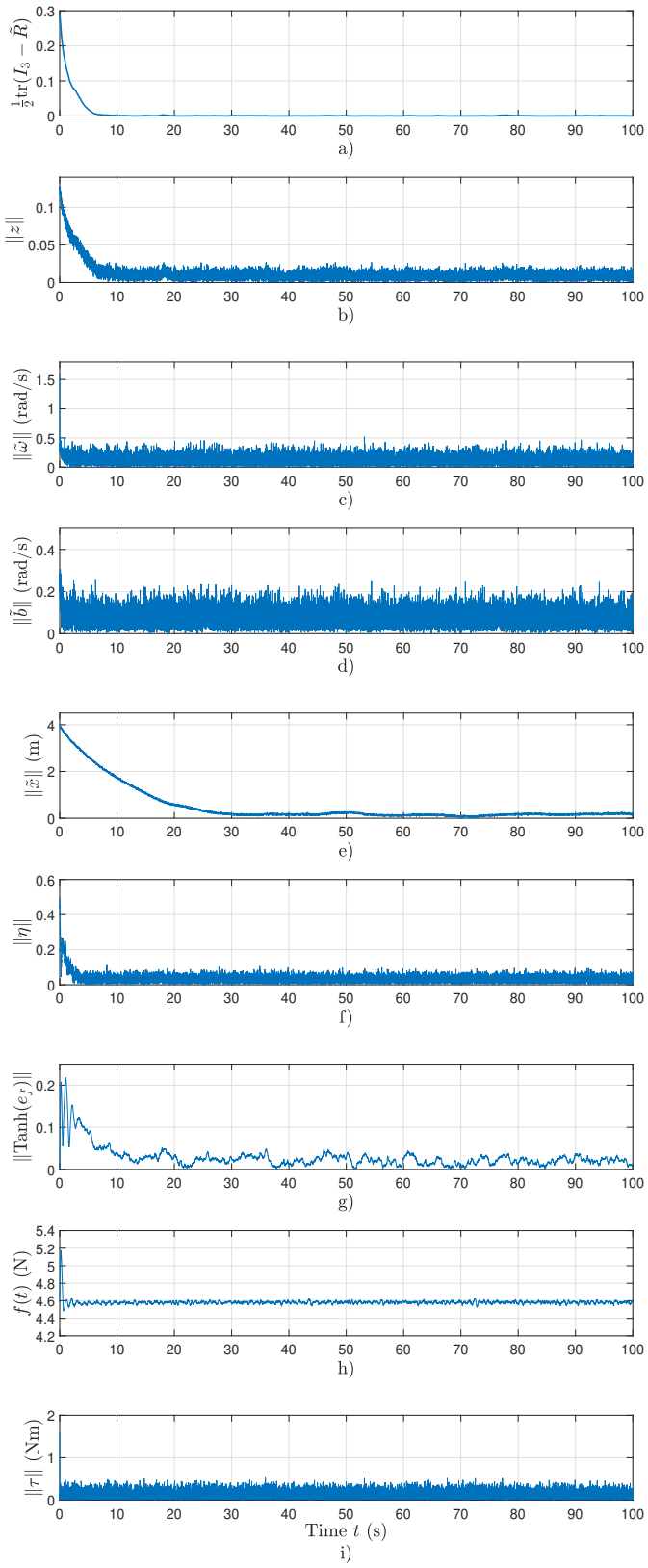

Fig. 4. Scenario 2 (noisy-measurement situation). Performance of the proposed controller under noisy measurements.

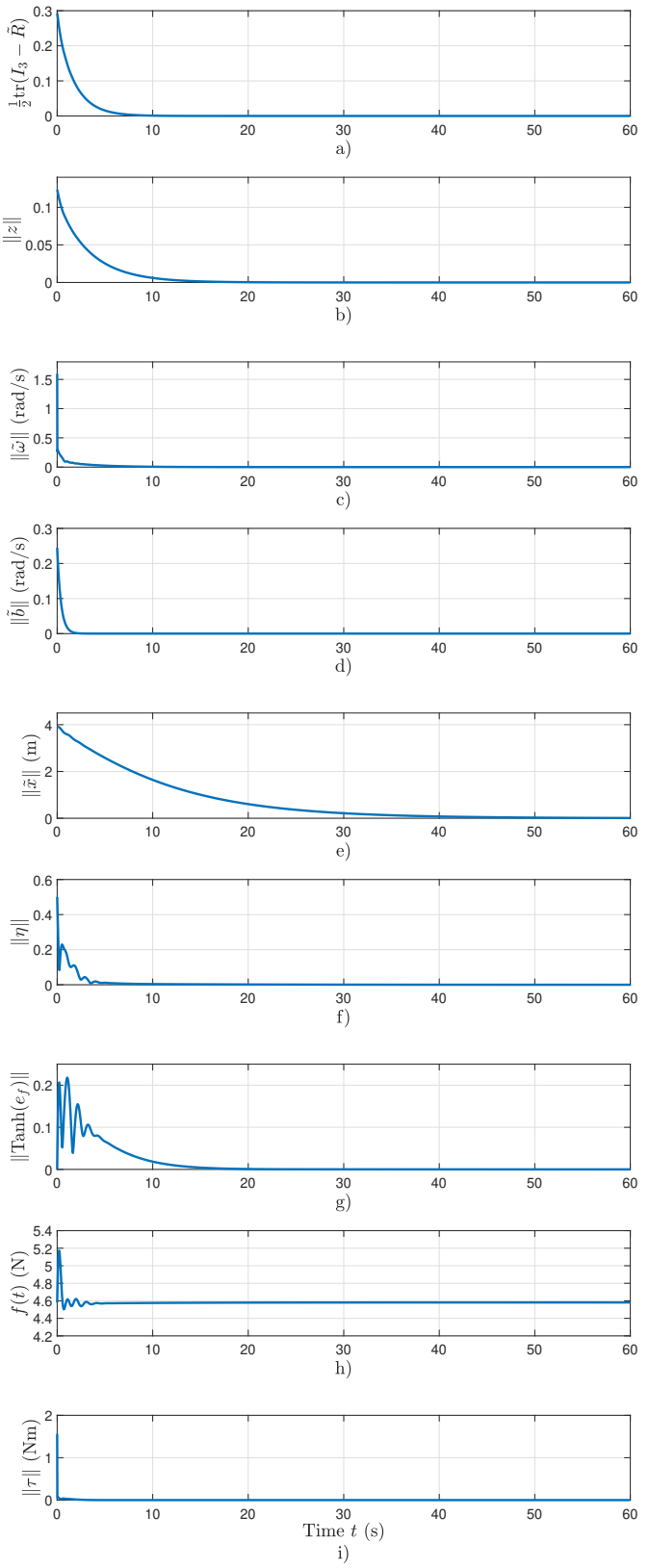

Fig. 5. Scenario 3 (uncertain inertia matrix). Performance of the proposed controller under uncertainty in the inertia matrix.

later, in view of (70)-(72), it can be written

$$\begin{aligned}\|R - R_d\| &\leq \|R - R_d\|_F = \|R^T - R_d^T\|_F \\ &\leq \|H_B - H_D\|_F \|H_I^T \bar{W}^{-1}\|_F \\ &= \sqrt{\mathrm{tr}\left(\left(H_B - H_D\right)^T \left(H_B - H_D\right)\right)}\end{aligned}$$

where the fact that $\mathrm{tr}(A) = \mathrm{tr}(A^T)$, and $\varpi := \mathrm{tr}\left(\bar{W}^{-1}\right) > 0$

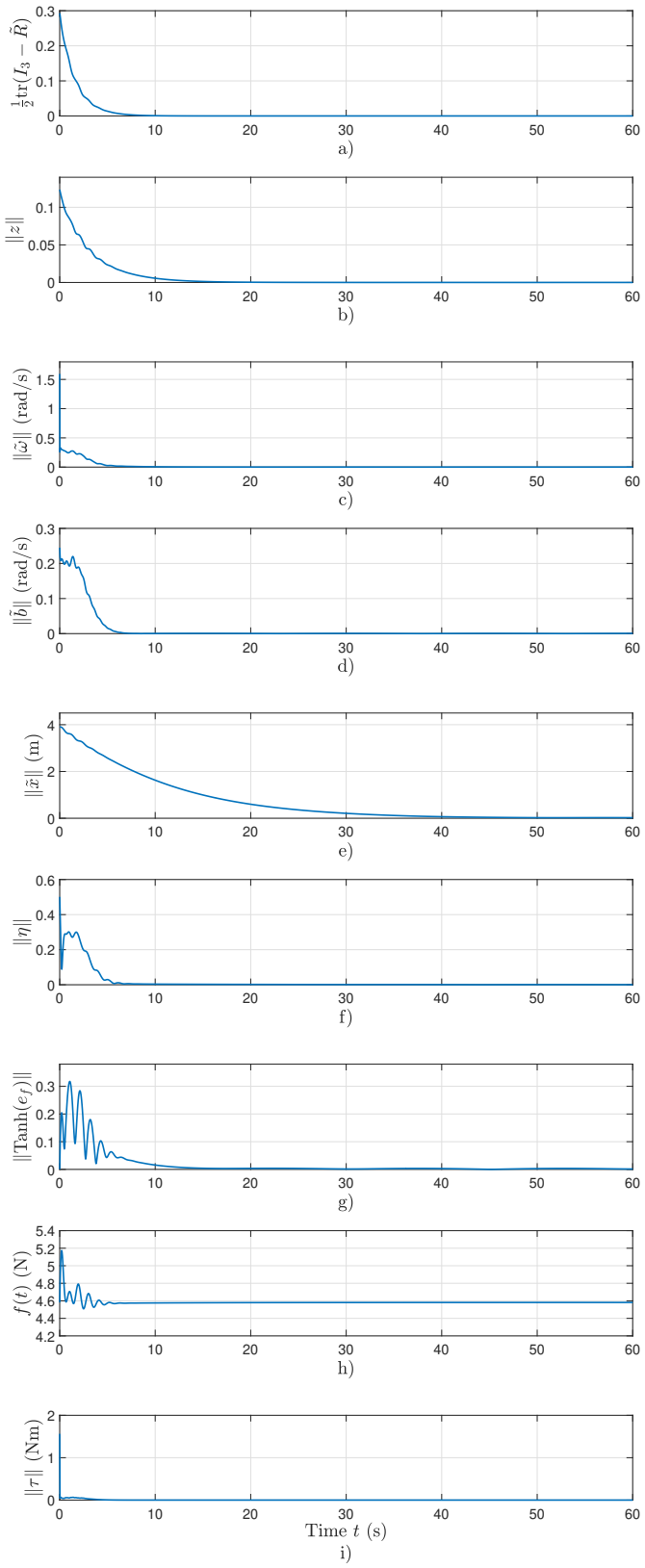

Fig. 6. Scenario 4 (Apparent acceleration). Performance of the proposed controller using an accelerometer.

were used. Therefore, according to (34), it yields

$$\|R - R_d\| \leq \sqrt{\frac{\varpi\beta}{\alpha_1}}\|z\|.$$

Pedro Casau a, Ricardo G. Sanfelice b, Rita Cunha a, David Cabecinhas c,a, Carlos Silvestre 2015

REFERENCES

[1] R. Mahony, V. Kumar, and P. Corke, "Multirotor aerial vehicles: Modeling, estimation, and control of quadrotor," *IEEE Robotics and Automation magazine*, vol. 19, no. 3, pp. 20–32, 2012.

[2] S. Grzonka, G. Grisetti, and W. Burgard, "A fully autonomous indoor quadrotor," *IEEE Transactions on Robotics*, vol. 28, no. 1, pp. 90–100, 2011.

[3] P. Serra, R. Cunha, T. Hamel, D. Cabecinhas, and C. Silvestre, "Landing of a quadrotor on a moving target using dynamic image-based visual servo control," *IEEE Transactions on Robotics*, vol. 32, no. 6, pp. 1524–1535, 2016.

[4] M.-D. Hua, T. Hamel, P. Morin, and C. Samson, "Introduction to feedback control of underactuated vtolvehicles: A review of basic control design ideas and principles," *IEEE Control systems magazine*, vol. 33, no. 1, pp. 61–75, 2013.

[5] F. Chen, W. Lei, K. Zhang, G. Tao, and B. Jiang, "A novel nonlinear resilient control for a quadrotor uav via backstepping control and nonlinear disturbance observer," *Nonlinear Dynamics*, vol. 85, no. 2, pp. 1281–1295, 2016.

[6] H. Liu, D. Li, Z. Zuo, and Y. Zhong, "Robust three-loop trajectory tracking control for quadrotors with multiple uncertainties," *IEEE Transactions on Industrial Electronics*, vol. 63, no. 4, pp. 2263–2274, 2016.

[7] Z. Zuo and C. Wang, "Adaptive trajectory tracking control of output constrained multi-rotors systems," *IET Control Theory & Applications*, vol. 8, no. 13, pp. 1163–1174, 2014.

[8] B. Zhao, B. Xian, Y. Zhang, and X. Zhang, "Nonlinear robust adaptive tracking control of a quadrotor uav via immersion and invariance methodology," *IEEE Transactions on Industrial Electronics*, vol. 62, no. 5, pp. 2891–2902, 2014.

[9] Y. Yu and X. Ding, "A global tracking controller for underactuated aerial vehicles: design, analysis, and experimental tests on quadrotor," *IEEE/ASME Transactions on Mechatronics*, vol. 21, no. 5, pp. 2499–2511, 2016.

[10] M.-D. Hua, T. Hamel, P. Morin, and C. Samson, "A control approach for thrust-propelled underactuated vehicles and its application to vtol drones," *IEEE Transactions on Automatic Control*, vol. 54, no. 8, pp. 1837–1853, 2009.

[11] A. Roberts and A. Tayebi, "Adaptive position tracking of vtol uavs," *IEEE Transactions on Robotics*, vol. 27, no. 1, pp. 129–142, 2010.

[12] T. Lee, M. Leok, and N. H. McClamroch, "Nonlinear robust tracking control of a quadrotor uav on se (3)," *Asian journal of control*, vol. 15, no. 2, pp. 391–408, 2013. Goodarzi13, PID,position control mode=ttitude mode=position controller

[13] D. Invernizzi and M. Lovera, "Trajectory tracking control of thrust-vectoring uavs," *Automatica*, vol. 95, pp. 180–186, 2018.

[14] S. Bertrand, N. Guénard, T. Hamel, H. Piet-Lahanier, and L. Eck, "A hierarchical controller for miniature vtol uavs: Design and stability analysis using singular perturbation theory," *Control Engineering Practice*, vol. 19, no. 10, pp. 1099–1108, 2011.

[15] L. Wang and H. Jia, "The trajectory tracking problem of quadrotor uav: Global stability analysis and control design based on the cascade theory," *Asian Journal of Control*, vol. 16, no. 2, pp. 574–588, 2014.

[16] A. Roza and M. Maggiore, "A class of position controllers for underactuated vtol vehicles," *IEEE Transactions on Automatic Control*, vol. 59, no. 9, pp. 2580–2585, 2014.

[17] A. Abdessameud and A. Tayebi, "Global trajectory tracking control of vtol-uavs without linear velocity measurements," *Automatica*, vol. 46, no. 6, pp. 1053–1059, 2010.

[18] T. Hamel, R. Mahony, R. Lozano, and J. Ostrowski, "Dynamic modelling and configuration stabilization for an x4-flyer." *IFAC Proceedings Volumes*, vol. 35, no. 1, pp. 217–222, 2002.

[19] P. Castillo, A. Dzul, and R. Lozano, "Real-time stabilization and tracking of a four-rotor mini rotorcraft," *IEEE Transactions on control systems technology*, vol. 12, no. 4, pp. 510–516, 2004.

[20] H. Rehbinder and B. K. Ghosh, "Pose estimation using line-based dynamic vision and inertial sensors," *IEEE Transactions on Automatic control*, vol. 48, no. 2, pp. 186–199, 2003.

[21] R. Mahony, T. Hamel, and J.-M. Pflimlin, "Nonlinear complementary filters on the special orthogonal group," *IEEE Transactions on automatic control*, vol. 53, no. 5, pp. 1203–1218, 2008.

[22] A. Roberts and A. Tayebi, "A new position regulation strategy for vtol uavs using imu and gps measurements," *Automatica*, vol. 49, no. 2, pp. 434–440, 2013.

[23] E. Espíndola and Y. Tang, "Attitude tracking for rigid bodies using vector and biased gyro measurements," *arXiv preprint*, 2022.

[24] A. Tayebi, A. Roberts, and A. Benallegue, "Inertial vector measurements based velocity-free attitude stabilization," *IEEE Transactions on Automatic Control*, vol. 58, no. 11, pp. 2893–2898, 2013.
[25] F. Zhang, D. M. Dawson, M. S. de Queiroz, and W. E. Dixon, "Global adaptive output feedback tracking control of robot manipulators," *IEEE Transactions on Automatic Control*, vol. 45, no. 6, pp. 1203–1208, 2000.
[26] H. K. Khalil, "Nonlinear systems third edition," *Patience Hall*, vol. 115, 2002.
[27] S. Sastry and M. Bodson, *Adaptive Control: Stability, Convergence and Robustness*. Courier Corporation, 2011.
[28] E. Espíndola and Y. Tang, "A new angular velocity observer for attitude tracking of spacecraft," *ISA transactions*, 2022.
[29] J. F. Guerrero-Castellanos, N. Marchand, A. Hably, S. Lesecq, and J. Delamare, "Bounded attitude control of rigid bodies: Real-time experimentation to a quadrotor mini-helicopter," *Control Engineering Practice*, vol. 19, no. 8, pp. 790–797, 2011.

Eduardo Espíndola received the Ph.D. degree in electrical engineering from the National Autonomous University of Mexico, in 2022. His main research activities include non-linear control applied to aerospace systems and rigid bodies.

Yu Tang received the Ph.D. degree in electrical engineering from the National Autonomous University of Mexico, in 1988, and then joined the same university. He held a research/teaching position at the University of California, Berkeley, in 1996, the Mexican Petroleum Institute, Mexico City, in 2002, and the University of Science and Technology of China, Hefei, China, in 2018. His academic interests include non-linear control and estimation with applications in mechatronics and aerospace engineering.